

Fan Mo\*, Anastasia Borovykh, Mohammad Malekzadeh, Hamed Haddadi, and Soteris Demetriou

# Layer-wise Characterization of Latent Information Leakage in Federated Learning

**Abstract:** Training deep neural networks via federated learning allows clients to share the model updated on their data, instead of the original data. In practice, it is shown that a client’s private information, unrelated to the main learning task, can be discovered from the shared model, which compromises the promised privacy protection. However, there is still no formal approach for quantifying the leakage of such latent information from the shared model/gradients. As a solution, we introduce and evaluate two mathematically-grounded metrics for better characterizing the amount of information included in the shared gradients computed on the clients’ private data. First, using an adaptation of the *empirical  $\mathcal{V}$ -information*, we show how to quantify the amount of private latent information captured in gradients that are usable for an attacker. Second, based on a *sensitivity analysis* using Jacobian matrices, we show how to measure changes in the gradients with respect to latent information. Further, we show the applicability of our proposed metrics in (i) localizing private latent information in a layer-wise manner, in both settings where we have or we do not have the knowledge of the attackers’ capability, and (ii) comparing the capacity of each layer in a neural network in capturing higher-level versus lower-level latent information. Experimental results on three real-world datasets using three benchmark models show the validity of the proposed metrics.

**Keywords:** Information Privacy, Deep Neural Networks, Federated Learning, Measurement.

---

\*Corresponding Author: **Fan Mo:** Imperial College London, E-mail: f.mo18@imperial.ac.uk

**Anastasia Borovykh:** Imperial College London, E-mail: a.borovykh@imperial.ac.uk

**Mohammad Malekzadeh:** Imperial College London, E-mail: m.malekzadeh@imperial.ac.uk

**Hamed Haddadi:** Imperial College London, E-mail: h.haddadi@imperial.ac.uk

**Soteris Demetriou:** Imperial College London, E-mail: s.demetriou@imperial.ac.uk

## 1 Introduction

Federated learning (FL) [1] allows *clients* to jointly train a model, *e.g.* a deep neural network (DNN), on their local data, and iteratively share their updates with a *server* that aggregates the received updates. Recently, there has been a surge of interest in FL [2–5], as a server can train a model on its clients’ data without the need for collecting their data in a centralized location, which in many cases is not possible due to computational costs, privacy risks, and even legal considerations [6].

However, sharing model updates is not a privacy panacea as the shared model can still leak private information [7]. Previous work has studied the privacy risks in sharing model parameters/gradients by constructing various attacks aimed at extracting private information. For example, data reconstruction attacks [8–10] aim to recover the original training data. Property inference attacks (PIA) [11–13] aim to infer the client’s private latent information (or property), *e.g.* gender or race. Membership inference attacks (MIA) [14, 15] aim to infer a client’s presence in the training phase.

Despite the abundance of empirical attacks on the client’s shared gradients [8–18], there is no comprehensive explanation or mathematically-grounded metrics for characterizing private information leakage in FL, especially for latent information. Previous work either focuses on explaining DNN behavior in *centralized* learning where only the final model parameters are analyzed [14, 15, 19, 20], or conducts gradient-based privacy measurements [17, 21] focusing on the original data. Original information is only clearly memorized in weak aggregation (several inputs such as 8 in one batch) [9, 17], but latent information can be captured in strong gradient aggregation (several batches of data) [12, 13]. A strong aggregation is a common practice in FL [1, 22]; the right tools to quantify attack successes and private latent information leakage in this setting are still lacking.

Although there are many works [23–28] on the memorization and generalization of DNNs *w.r.t.* the main task (*e.g.* classification) that DNNs are trained on, these works are not able to explain the memorization of latent information that is independent of the main task.

Moreover, these works are mostly limited to explaining *shallow NNs* [25], as it is shown that is much harder to theoretically formulate memorization of *deeper NNs*; because the memorization made via backward propagation throughout the DNN is still not fully understood [23, 24, 28]. Therefore, there has been a surge of interest in conducting layer-wise analyses for understanding the learned representation by a DNN [29, 30] or to characterize the information flow in a DNN [31–33]. However, these layer-wise investigations only provide insights on how information evolves during *forward propagation*. Hence, there is a need for localization and quantification of information memorization incurred by *backward propagation*. Moreover, due to the current lack of understanding into *where* the private information is, existing defenses are too coarse-grained leading to compromises in either the model utility or the protection performance. For example, most existing privacy-preserving techniques (*i.e.* differential privacy (DP) [34, 35] or fully homomorphic encryption (FHE) [36]) apply to the complete model without considering whether parts of the model may be more sensitive and should be the protection priority.

**Our work** aims to fill these gaps and take a concrete step towards quantifying and localizing latent information in FL. Specifically, we aim at answering the question: what type of latent information is captured *where* in the neural network? We argue that localizing the latent information captured in a DNN’s layers can help in the better design of flexible and robust defenses against model parameter/gradient-based attacks. By understanding and quantifying where the private information is, layer-wise characterization can help adjust the granularity of the defense mechanism.

We elaborate on the severe and open problem *i.e.* how property inference attacks [13] leverage latent information present in the computed gradients, and why the well-known Shannon mutual information [37] and the data processing inequality cannot properly quantify such information leakage. To solve this problem, we propose adopting a different notion of information, *V-information* [38], also known as ‘usable’ information. We show that *V-information* can measure the layer-wise latent information privacy risk and explain which layers are the most vulnerable to a property inference adversary targeting specific properties. Moreover, as *V-information* needs knowledge of the specific class of attack models, we further present a second metric based on a *sensitivity analysis* of the gradients *w.r.t.* latent information, which is more suitable when modeling a

generic adversary. To validate the proposed metrics we use three benchmark DNN architectures that are suitable for edge-devices using real-world datasets, and compare them against the success rates of property inference attacks where the adversary gains access to the gradients of only a specific layer.

We find that both *V-information* and sensitivity exhibit strong correlations with the layer-wise adversary’s success rate (establishing predictive validity), and conclude that these metrics can accurately localize the private information in DNN layers. Our empirical evaluation and analysis unveil unique insights into the model: in a typical DNN that consists of convolutional layers followed by fully connected layers in the end (*e.g.* VGG [39]), the first fully connected layer captures the largest amount of private property information of the client’s data. The proposed metrics and insights significantly advance our current understanding of latent information leakage in FL.

**Our contributions** are summarized below.

- To the best of our knowledge this work is the first to characterize private latent information in shared models/gradients *at a layer granularity* during the training phase in FL.
- We adopt *V-information* theory to explain and measure a property inference adversary’s success rate on a specific target property given a specific attack.
- We define and analyze a generic, *i.e. model- and property-independent*, sensitivity metric that is an easy-to-use alternative to *V-information* for quantifying latent information leakage of each layer.
- We empirically validate the success of the metrics through a correlation analysis with the attack success rate.

**Paper organisation.** Section 2 discusses related work, while Section 3 defines the target privacy problem. Section 4 presents our information theoretical privacy analysis and proposed privacy metrics. Sections 5 and 6 describe the setup and results of our empirical predictive validation of the proposed metrics. Lastly, Section 7 discusses main insights from our work, and Section 8 concludes the paper.

## 2 Background

**Notations.** We first present the notations used throughout the paper. We use lower-case italic, *e.g.*  $x, y$ ,

for deterministic scalar values; lower-case bold italic, *e.g.*  $\mathbf{x}, \mathbf{y}$ , for deterministic vectors; upper-case bold italic, *e.g.*  $\mathbf{X}, \mathbf{Y}$ , for deterministic matrices. We use lower-case normal, *e.g.*  $x, y$ , for instances of a random variable, and upper-case normal, *e.g.*  $X, Y$ , for random variables of any dimensions.

## 2.1 Privacy risks in federated learning

**Federated Learning.** FL is a machine learning technique where multiple clients, *e.g.* smartphone users [1] or health organizations [40], collaboratively train a model under the orchestration of a central server while keeping the training data at the client’s side [2]. Each client trains a model on its own data and then shares the model, instead of the original data. The server aggregates the received updates from multiple clients, *e.g.* by simply averaging them into a *global model* [1]. Then, the server broadcasts the global model back to clients, such that clients can fine-tune the model on their data again and repeat the process until convergence.

A key hyperparameter in FL configurations is the number of steps (*i.e.* local epochs) that clients train the model at each round (*i.e.* global epoch). If the model is only trained on one batch of data (*i.e.* one step) and then it is sent back to the server, the FL is regarded as using Federated SGD (FedSGD) approach; otherwise, when the model is locally updated multiple times on multiple batches of data, then it is regarded as Federated Averaging (FedAvg) [1]. Targeting a specific accuracy for the model on a validation dataset, FedAvg usually reduces communication rounds between clients and the server, but leads to a larger number of total local epochs on each client, compared to FedSGD. In addition, because FedSGD has weaker aggregation in terms of gradients (*i.e.* only one batch of clients’ data), it becomes more vulnerable to adversaries who aim at revealing the client’s private data [9, 10, 13].

**Attacks based on Gradients.** Previous works showed how an adversary can *reconstruct the input data* based on its corresponding gradients [9, 10]. The attacker randomly initializes dummy data and feeds it into the model in order to get dummy gradients. By optimizing the dummy gradients to get close to the real original gradients, the dummy data gets close to the real private data. Experiments [9] showed the data construction can reach pixel-wise accuracy for images and token-wise matching for texts. However, the attack tends to fail when the aggregation of gradients is sufficient (*e.g.* the

batch size is larger than 8) or the data has high dimension (*e.g.* images resolution is larger than  $64 \times 64$ ) because the optimization becomes hard to solve when more variables are involved [9, 18]. Other attacks, the property inference attack (PIA) [13] and membership inference attack (MIA) [12], focus on extracting latent private information, *i.e.* a specific property of the client or the presence of a specific client. The attacker collects multiple model updates and feeds its own data with or without one target property to these models to obtain the corresponding gradients. The gradients with their property labels are used to train a binary classifier which can distinguish whether a set of gradients obtained from other clients has this property or not. Compared to data reconstruction, PIAs are more successful in a wider range of problems as the effect of aggregation is limited. High-level properties are easier to capture than high dimensional data at pixel-level. In addition, the gradients to be aggregated may contain the same property information.

**Privacy Analysis.** A previous work [21] indicates that the gradients of the first layer are proportional to the original data such that they can help to reconstruct the input data. Another work [9] shows the last layer has the smallest loss between the dummy and real gradients in data reconstruction. These results may not be suitable for comparison across layers since the calculation of loss depends on the layer sizes which could be different. A similar layer-wise analysis [13] also includes the T-distributed Stochastic Neighbor Embedding (t-SNE) [41] projection: a dimensionality reduction on layers’ outputs which allows to visually explain why inference attack can exploit unintended property information. The results show that feature vectors are grouped by properties in the former layers and by the class label in the latter layer. However, this analysis is on the layers’ activation (in forward propagation) instead of gradients (produced in backward propagation), and the latter one is what clients share with the server and thus could be exploited by adversaries. In addition, another proposed framework utilizes the data reconstruction attack to measure the privacy leakage from gradients [17], but this analysis is restricted to this particular attack and cannot be extended to privacy measurement on high-level features.

## 2.2 Shannon mutual information and $\mathcal{V}$ -information

**Shannon MI and information flow in DNNs.** A well-known metric for quantifying the information flow of the training dataset in a DNN’s forward propagation is the Shannon mutual information (MI) [31, 33, 37]. For an observed data  $X$ , with the label  $Y$ , the DNN performs layer by layer computations on  $X$  (from layer 1 to layer  $L$ ) to provide prediction,  $\hat{Y}$ , which forms a Markov chain:  $Y \rightarrow X \rightarrow T_1 \cdots \rightarrow T_L \rightarrow \hat{Y}$ , where  $T_l$  refers to representation in layer  $l$  (please refer to Section 3.1 for **notations** details). Then, the MI between  $X$  (or  $Y$ ) and  $T_l$  satisfies the Data Processing Inequality (DPI) [31, 32, 42],

$$\begin{aligned} I(X; T_1) &\geq I(X; T_2) \cdots \geq I(X; T_L) \geq I(X; \hat{Y}), \\ I(Y; T_1) &\geq I(Y; T_2) \cdots \geq I(Y; T_L) \geq I(Y; \hat{Y}). \end{aligned}$$

These inequalities correspond to the intuition that information should *not* increase during the layer-by-layer forward propagation in DNNs. However, DPI fails to explain the backward propagation because the Markov chain construction on inputs, model parameters, and computed *gradients* is much more complex than that in the forward propagation (see Figure 1). In other words, the computed gradients at each layer not only depend on the output of the previous layer but also depend on the computed gradients of the next layer and etc.

More specifically, one could reasonably expect a DNN to extract features that are useful for the target task, so that ‘usable’ information for the task  $Y$  memorized in DNN parameters/gradients would be *increasing* throughout the layers [38]. This intuition has been verified by analyzing the forward propagation: intermediate representations (*e.g.*  $T$ ) of the earlier layers contain more generic features that are useful for many tasks, but later layers become progressively more specific to the details relevant to the desired task [33, 43]. However, there is no successful MI analysis directly on gradients produced in the backward propagation.

**$\mathcal{V}$ -information.** One difficulty of using MI to analyze model gradients is the bias of MI estimators on high-dimensional random variables (*e.g.*  $T$  and  $Y$ ) with unknown distribution [32, 44, 45]. A further difficulty is that the Shannon MI assumes no computational constraints [38], and under the assumption of unbounded computational power, each  $T_l$  allows one to extract as much information about  $Y$  as quantified by the MI between them.

However, in practice this is difficult (or even impossible) to achieve even using state-of-the-art techniques such as deep learning (*i.e.* with limited computational power). The computational constraints can be made precise through the concept of  $\mathcal{V}$ -information [38] defined as,

$$\begin{aligned} I_{\mathcal{V}}(X \rightarrow Y) &= \inf_{f \in \mathcal{V}} \mathbb{E}_{y \sim Y} [-\log f[\emptyset](y)] \\ &\quad - \inf_{f \in \mathcal{V}} \mathbb{E}_{x, y \sim X, Y} [-\log f[x](y)] \end{aligned} \quad (1)$$

where  $X$  and  $Y$  are random variables taking values in  $\mathcal{X} \times \mathcal{Y}$  and  $\mathcal{V}$  is a predictive family (*i.e.* a set of algorithms or models that one can use representing the computational constraints). Here  $f[\emptyset]$  (or  $f[x]$ ) represents a probability measure on  $Y$  without side-information (or with side-information  $x$ ). The  $f[\cdot](y)$  is the value of the corresponding density evaluated at  $y$ . The  $I_{\mathcal{V}}(X \rightarrow Y)$  represents the change in the predictability of an output  $Y$  given side information  $X$  using models from  $\mathcal{V}$ . We can then apply the  $\mathcal{V}$ -information to analyze the information contained in the layers of a DNN and show that under computational constraints the latter layers’ parameters or gradients may contain latent information which is easier to interpret by adversaries for inferring privacy-sensitive information such as property, which provides theoretical validation on privacy risks of layer’s gradients.

## 2.3 Sensitivity

**Sensitivity and privacy.** Understanding the private information memorization by DNNs is somehow related to the explanation of the learning capability and the generalization ability of DNNs; something that is still an active area of research [24, 28]. The main assumption is that learning a model that generalizes well avoids the memorization of unnecessary information [19]. One predictive factor of model generalization is sensitivity [46, 47]. *Sensitivity* is a concept used for analyzing DNNs which quantifies to what extent the target (*i.e.* output) variables are affected by small changes in the corresponding input variables. Hypothesizing that low sensitivity is directly related to less memorization of private information, privacy threats of sharing model parameters can be smaller as changes in the parameters are harder to be noticed by adversaries or attackers.

Sensitivity has also been applied in measuring model robustness on adversarial example attacks [48, 49]. This follows the intuition that a model that is non-sensitive to certain changes in inputs, is expected

to have high robustness. Similarly, sensitivity, which is used to quantify the maximum difference between two adjacent datasets [50, 51], is a crucial aspect of applying DP for privacy guarantees. DP can also certify model robustness to adversarial examples by correlating the sensitivity with the norm (1,2, and  $\infty$ ) of adversarial attacks [52].

**Measuring sensitivity.** One measure for the sensitivity used in DNNs is the norm of the input-output Jacobian, *i.e.* the Jacobian matrix of class probabilities *w.r.t.* the input [46, 47]. It reflects the changes in the DNN output as the input is perturbed or changed. More specifically, given a model  $f$  mapping input  $\mathbf{x}$  to output probabilities  $\mathbf{y}$ , the input-output Jacobian is computed as,

$$\mathbf{J}(\mathbf{x}) = \frac{\partial \mathbf{y}}{\partial \mathbf{x}} = \frac{\partial f(\mathbf{x})}{\partial \mathbf{x}}. \quad (2)$$

Then by adopting the Frobenius norm of Jacobian one can measure sensitivity [47] using,

$$\mathbb{E}_{\mathbf{x}}[\|\mathbf{J}(\mathbf{x})\|_F], \quad (3)$$

where the expected value is typically approximated by a summation over the sample data points, *e.g.* one dataset  $\mathbf{x}_K$  with  $K$  samples.

It is worth noting that the use of the Frobenius norm is sensible here since in this application the sensitivity is measured over a single task and its corresponding probability output (*e.g.* outputs of softmax functions) [47]. However, other norms may be considered when matrix sizes or magnitudes are different in order to make the metric comparable across tasks or models.

## 3 Problem Formulation

In this section, we formulate the problem by defining the notion of privacy as considered in this work and describing the adversary who aims to disclose this type of privacy. We also revisit how the privacy issue arises based on gradient computation and sharing in FL.

### 3.1 Privacy definitions

We aim at characterizing the *property privacy* in shared gradients/models, as oppose to *input privacy*. In federated learning (as well as other ML paradigms that require sharing training data/models), input privacy refers to the privacy of the training data [3, 8, 9, 13, 53]. Here we focus on the property privacy of input data,

*e.g.* whether this input has one property or not, as the property is high-level latent information which aggregation gradients can easily carry, and the property privacy is more difficult to preserve than input privacy in FL. In particular, let  $\mathbf{X}$  denote one individual client’s original data (considered to be private) used in the training phase and let  $\mathbf{p}$  denote the property of the data. The input privacy risk is measured by how much information about  $\mathbf{X}$  an adversary can extract, and the property privacy risk is measured by how much information about  $\mathbf{p}$  an adversary can extract from the gradients which are shared during training. The goal of property inference attack such as [13] is to extract information about  $\mathbf{p}$  from gradients.

### 3.2 Gradient computation

We first revisit how gradients are computed as a function of the input to which later shows the root cause for how a gradient  $\mathbf{G}$  can reveal input data  $\mathbf{X}$  and information about the property  $\mathbf{p}$ . Let  $\mathbf{X} = [\mathbf{x}_1, \dots, \mathbf{x}_K]$  be one batch of data consisting of  $K$  samples from client  $c$ ’s training dataset  $\mathcal{X}^c$ , and let  $\mathbf{Y} = [\mathbf{y}_1, \dots, \mathbf{y}_K]$  be the corresponding ground truth (*e.g.* labels for a classification task). The complete training dataset of all  $C$  clients is denoted by  $\mathcal{X} = \{\mathcal{X}^1, \dots, \mathcal{X}^C\}$ . For a DNN model with  $L$  layers, we denote layer  $l$ ’s parameters with  $\mathbf{W}_l$  and  $\mathbf{b}_l$ ; the weights and biases, respectively. In the *forward propagation* from layer 1 to  $L$ , the layer  $l$  computes

$$\mathbf{A}_l = [\mathbf{a}_{l,1}, \dots, \mathbf{a}_{l,K}] = \mathbf{W}_l \mathbf{T}_{l-1} + \mathbf{b}_l \mathbf{1}^\top,$$

where  $\mathbf{W}_l \in \mathbb{R}^{N_l \times N_{l-1}}$ ,  $\mathbf{T}_{l-1} = [\mathbf{t}_{l-1,1}, \dots, \mathbf{t}_{l-1,K}] \in \mathbb{R}^{N_{l-1} \times K}$ ,  $\mathbf{b}_l \in \mathbb{R}^{N_l}$ ,  $\mathbf{1} \in \{1\}^K$ .  $N_l$  denotes the size (*i.e.* the number of neurons) of the layer  $l$ , and  $\mathbf{T}_{l-1}$  shows the *intermediate representation* that is the output of the (previous) layer  $l-1$ , and  $\mathbf{t}_{l-1,k}$  corresponds to one sample  $k$ ’s outputs. Then, the layer  $l$ ’s output is  $\mathbf{T}_l = [\sigma(\mathbf{a}_{l,1}), \dots, \sigma(\mathbf{a}_{l,K})] \in \mathbb{R}^{N_l \times K}$ , denoted as  $\sigma(\mathbf{A}_l)$  for simplicity, where  $\sigma(\cdot)$  is the chosen activation function. Note that  $\mathbf{T}_0 = \mathbf{X}$  and  $\mathbf{T}_L = \hat{\mathbf{Y}}$  the prediction on ground truth.

In the *backward propagation*, the loss  $\ell$  between  $\hat{\mathbf{Y}}$  and  $\mathbf{Y}$  propagates from the layer  $L$  to 1. For layer  $l$ , the gradient vector  $\mathbf{G}_l$  consists of the gradients of the weights and biases  $\{\mathbf{G}_l^{(w)}, \mathbf{G}_l^{(b)}\}$ , which are computed using chain rule:

$$\mathbf{G}_l^{(w)} = \frac{\partial \ell}{\partial \mathbf{W}_l} = \frac{\partial \ell}{\partial \mathbf{A}_l} \frac{\partial \mathbf{A}_l}{\partial \mathbf{W}_l} = \frac{\partial \ell}{\partial \mathbf{A}_l} \mathbf{T}_{l-1}^\top \quad (4)$$

$$\mathbf{G}_l^{(b)} = \frac{\partial \ell}{\partial \mathbf{b}_l} = \frac{\partial \ell}{\partial \mathbf{A}_l} \frac{\partial \mathbf{A}_l}{\partial \mathbf{b}_l} = \frac{\partial \ell}{\partial \mathbf{A}_l} \mathbf{1} \quad (5)$$

where  $\mathbf{G}_l^{(w)} \in \mathbb{R}^{N_l \times N_{l-1}}$  and  $\mathbf{G}_l^{(b)} \in \mathbb{R}^{N_l}$  and have the same size with  $\mathbf{W}_l$  and biases  $\mathbf{b}_l$  respectively.

The set of all layers'  $\mathbf{G}^{(w)}$  and  $\mathbf{G}^{(b)}$  in Equation 4 and 5 is the minimum unit to update in FL, *i.e.* corresponding to the FedSGD.  $\mathbf{G}^{(w)}$  and  $\mathbf{G}^{(b)}$  are also targeted by adversaries to extract private information of  $\mathbf{X}$  or its sub-information *e.g.*  $\mathbf{p}$ . In FedAvg, before updating, more batches of data are fed for training, and the gradients of multiple batches are aggregated together element-wisely by

$$\sum_{\mathbf{x}_i \in \mathcal{X}^c} \{\mathbf{G}_l^{(w)}\}_{\mathbf{x}_i}; \sum_{\mathbf{x}_i \in \mathcal{X}^c} \{\mathbf{G}_l^{(b)}\}_{\mathbf{x}_i} \quad (6)$$

### 3.3 Adversary model

**Adversary  $\mathcal{A}$**  (Property Inference): The adversary aims to disclose private information of clients by observing updated gradients or global models broadcast from the server. We consider an adversary present on a FL participating node (*i.e.* one client) who aims to disclose private information of other clients by observing updated gradients or global models broadcast from the server. Based on the updated gradients/models,  $\mathcal{A}$  can infer the client's properties irrelevant to the prediction tasks of FL using property inference attacks [13]. To conduct the attack,  $\mathcal{A}$  first needs to observe multiple snapshots of the global model from the server and collects other information including auxiliary data about the property. The auxiliary data can be its own data or public data so they are easy to collect. By training a (binary) *classifier* utilizing the client's auxiliary data and the global model,  $\mathcal{A}$  is able to classify an updated gradient, which can be obtained by subtracting two sequential global models, as having the target property or not in corresponding inputs (see Section 2 or [13] for more details on PIAs). For example, the task of FL is to train a global model to classify gender based on clients' face images, and  $\mathcal{A}$  will infer one's shared gradient (produced by training the model with face images) as having a specific property of race (*e.g.* white or black, etc) or not.

## 4 Privacy Analysis and Metrics

### 4.1 General analysis on gradients' privacy risks

We first directly analyze how  $\mathbf{G}$  leaks information of  $\mathbf{X}$  or  $\mathbf{p}$  based on Equation 4, 5, and 6. Three *indi-*

*cations* for information leakage from DNN parameters (*i.e.* gradients) are: (1) One can obtain the layer  $l$ 's input ( $\mathbf{T}_{l-1}$ ) based on this layer's gradient updates. Because the first layer's input (*i.e.*  $\mathbf{T}_0$ ) is  $\mathbf{X}$ , the original input is highly likely to be leaked, which has been shown in previous research [21]. (2) Batch-based SGD (*i.e.* Mini-batch) reduces the potential leakage on one specific data sample  $\mathbf{x}_i, i \in 1, \dots, K$ , because gradients are computed over all samples in one batch (see Equation 4 and 5). Aggregation, *i.e.* the summation of gradients over multiple batches, also reduces the potential leakage (see Equation 6). (3) The term  $\frac{\partial \ell}{\partial \mathbf{A}_l} = \frac{\partial \ell}{\partial \mathbf{T}_l} \odot \sigma'(\mathbf{a}_l) = \mathbf{W}_{l+1}^\top \frac{\partial \ell}{\partial \mathbf{A}_{l+1}} \odot \sigma'(\mathbf{A}_l)$  (note that  $\odot$  is the Hadamard product), indicating that the gradient can potentially contain information of  $\mathbf{A}_l, \mathbf{W}_{l+1}, \mathbf{b}_{l+1}$ , and parameters of following layers (*i.e.*  $\mathbf{A}_{l+1}, \dots, \mathbf{A}_L$ ). However, the DPI (from layer 1 to  $L$ ) indicates that  $\mathbf{T}_{l+1}$  (or  $\mathbf{a}_{l+1}$  here) cannot contain more information on  $\mathbf{X}$  than  $\mathbf{T}_l$  (or  $\mathbf{a}_l$ ) in *forward propagation* [31, 32, 42].

**Backward Markov chain.** Similar to the Markov chain in the forward propagation, here we present the Markov chain in *backward propagation* from layer  $L$  to layer 1 based on how gradients are computed to clarify the information leakage from gradients. As shown in Figure 1,  $\mathbf{G}_l$  is produced based on layer  $l$ 's weights, biases, the previous representation, and next gradient (denoted by  $\mathbf{W}_l, \mathbf{b}_l, \mathbf{T}_{l-1}$ , and  $\mathbf{G}_{l+1}$ ). Previous research [31, 32] has indicated that, due to the data processing inequality,  $\mathbf{T}_l$  contains more information about  $\mathbf{X}$  than  $\mathbf{T}_k$  with  $k > l$ . Furthermore, matrix  $\mathbf{W}_l$  and  $\mathbf{b}_l$  are linearly aggregated gradient updates from multiple previous  $\mathbf{G}_l$  (*i.e.* the model parameters  $\boldsymbol{\theta}_t \leftarrow \boldsymbol{\theta}_{t-1} - \mathbf{G}_t$  for the  $t^{\text{th}}$  batch data), so intuitively  $\mathbf{W}_l$  and  $\mathbf{b}_l$  possibly not contain more information on  $\mathbf{X}$  than  $\mathbf{G}_l$ , and then the information of  $\mathbf{X}$  in  $\mathbf{T}_{l-1}$  may reflect that of  $\mathbf{X}$  in  $\mathbf{G}_l$ . See Appendix 9.1 for more analyses of estimating information on  $\mathbf{T}$ .

Moreover, related to indication (2), when it comes to a particular  $\mathbf{x}$ ,  $\mathbf{W}$  and  $\mathbf{B}$  can be regarded as less sensitive if they have been updated based on the complete dataset  $\mathcal{X}$ . We further argue that the attempt on evaluating gradient leakage on original data  $\mathbf{x}_i, i \in 1, \dots, K$ , such as [17], could be very limited and constrained under weak aggregation, *i.e.* a small batch size [9]. We refer to Appendix 9.2 for data reconstruction attack results on  $\mathbf{G}$ , which shows the first layer could be the most sensitive in terms of original data.

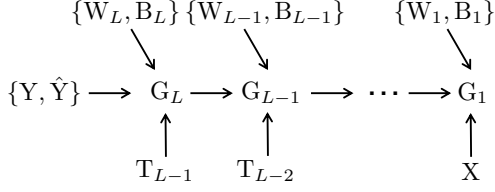


**Fig. 1.** Markov chain from layer  $L$  to layer 1 when producing gradients ( $G$ ) based on weights ( $W$ ), biases ( $B$ ), and intermediate representations ( $T$ ) in backward propagation (Note:  $\hat{Y}$  is  $T_L$ , and  $X$  is  $T_0$ ).

## 4.2 Privacy risk on high-level features

In more common FL scenarios the network parameters have sufficient aggregation since a relatively large batch size has been used or the loss is computed over multiple batches from one or even more clients (*e.g.* FedAvg). This kind of aggregation of data samples is likely to reduce the privacy risk on original data  $X$  or a specific  $x_i$  [9], as the aggregation may make it more difficult to precisely reconstruct higher dimensional information (*i.e.* input data). This pushes adversaries to move towards inferring *joint* properties across data of one individual such as the sensitive property of one batch data when corresponding gradients are shared.

**Estimator based on  $\mathcal{V}$ -information.** As claimed in [38], Shannon MI, due to its assumption of unbounded computational power, fails to explain that the ‘usable information’ in later layers of a DNN model may be higher than in initial layers. Instead, in our work, we ground our analysis in  $\mathcal{V}$ -information theory which we argue is better suited for analyzing the latent information captured in gradients, at the granularity of each of the layers of a DNN.

We consider the following setting: a computationally bounded agent, here a property inference adversary, is trying to predict the outcome of a real-valued random variable either with some side (or auxiliary) information or with no side information. The attacker, due to computational constraints, only has access to the attack models (denoted as  $f_{\mathcal{A}}$ ) from the predictive family  $\mathcal{V}_{\mathcal{A}}$ . We consider the threat model as defined in Section 3.3 where the adversary is able to obtain a gradient from a trained model and tries to distinguish whether this gradient was computed over a dataset which did or did not contain a certain property.

Let  $P$  and  $G_l$  be the presence of the property and the layer  $l$ ’s gradients, taking values in the sample space  $\{0, 1\} \times \mathbb{R}^{N_l \times N_{l-1}}$ , with  $N_l \times N_{l-1}$  denoting the dimensionality of used gradients. Let  $g_l$  denote an instance

of  $G_l$ . Then  $f_{\mathcal{A}}[g_l] \in \mathcal{P}(\{0, 1\})$  is a probability measure on  $\{0, 1\}$  chosen using the side information  $g_l$  and  $f_{\mathcal{A}}[g_l](p) \in \mathbb{R}$  is the value of the density evaluated at  $p \in \{0, 1\}$ . We assume that the predictive family satisfies the optional ignorance condition from Definition 1 in Appendix 9.3. Specifically, under certain assumptions a DNN and a random forest (RF) can satisfy this.

Let  $\mathcal{D}$  be the dataset where  $g_l, p \in \mathcal{D}$ . Let  $p_i \in \{0, 1\}$  denote whether or not the property is present for data sample  $i$  and let  $g_{l,i}$  the obtained layer  $l$ ’s gradients for data sample  $i$ . The empirical  $\mathcal{V}$ -information from  $G_l$  to  $P$  is defined as

$$\begin{aligned} \hat{I}_{\mathcal{V}_{\mathcal{A}}}(G_l \rightarrow P; \mathcal{D}) &= \inf_{f_{\mathcal{A}} \in \mathcal{V}_{\mathcal{A}}} \frac{1}{|\mathcal{D}|} \sum_{p_i \in \mathcal{D}} -\log f_{\mathcal{A}}[\emptyset](p_i) \\ &\quad - \inf_{f \in \mathcal{V}_{\mathcal{A}}} \frac{1}{|\mathcal{D}|} \sum_{g_{l,i}, p_i \in \mathcal{D}} -\log f_{\mathcal{A}}[g_{l,i}](p_i). \end{aligned} \quad (7)$$

Let  $z$  be the output of the attackers’ model. The density evaluated at  $p_i$  is then given by a softmax of the model output  $f[g_l]$  as follows:

$$f_{\mathcal{A}}[g_{l,i}](p_i) = \frac{e^{\{z(g_{l,i})\}_{p_i}}}{e^{\{z(g_{l,i})\}_0} + e^{\{z(g_{l,i})\}_1}}, \quad (8)$$

where  $f_{\mathcal{A}}[\emptyset](p_i) = \frac{1}{2}$ , the uniform distribution over the outputs. We then can use the  $\mathcal{V}$ -information to measure how well the presence of a property can be predicted when the adversary has access to one layer’s gradients as the side information. When  $f_{\mathcal{A}}[g_l]$  produces a perfect prediction with a loss equal to 0 on  $\mathcal{D}$ , the second item in Equation 7 is equal to 0 and consequently  $\mathcal{V}_{\mathcal{A}}$  achieves the highest  $\mathcal{V}$ -information between  $G$  and  $P$ . In the worst case,  $f_{\mathcal{A}}[g_l]$  produces a random prediction regardless of whether we use or not use side information  $g_l$  so the smallest  $\mathcal{V}$ -information is equal to 0.

In our setting the predictive family is the attacker’s model. To achieve the Infimum over  $\mathcal{V}_{\mathcal{A}}$ , we choose the attack model with the best performance, which by [13] is the best random forest. It is essential to evaluate the prediction results in probability density [38]; therefore we apply a softmax function during inference of the RF. DNNs usually have a softmax function at the end by default; however, they do not represent the best attack models as shown in [13]. For more information on the  $\mathcal{V}$ -information we refer to Appendix 9.3.

## 4.3 Privacy risk estimator based on sensitivity

The downside of  $\mathcal{V}$ -information is that it relies on certain assumptions about the model of the adversary, in

particular the predictive model  $\mathcal{V}$ . It may be of interest to directly compute privacy risk information for a *general* attacker, using solely the gradient information without making explicit assumptions about the attackers’ model. We will therefore utilize sensitivity to directly analyze the privacy risk on gradients *w.r.t.* high-level features (*e.g.* property).

For a PIA as in [13], the success of the attack lies in the ability of the classifier to distinguish between whether a certain gradient was computed over data that did or did not have a certain property. Intuitively, if certain gradients are non-sensitive to the input data or property in the data, the success of the attack can be expected to be low. This is due to the fact that in this case different input data or properties will not result in significantly different layer gradients. Training a classifier that would be highly successful in distinguishing between gradients with or without a certain property will then be non-viable.

We utilize the Jacobian matrix of the gradients as a straightforward *sensitivity* metric (similar to input-output Jacobian in [47] and [46]) for measuring the general privacy risk. the Jacobian of gradients *w.r.t.* one output  $\mathbf{y}$  is calculated. We expect the evaluation *w.r.t.*  $\mathbf{p}$  to be similar to that on  $\mathbf{y}$ , since both of them are high-level features, and the PIA can be achieved by having either the property task (*i.e.*  $\mathbf{p}$ ) or the main task (*i.e.*  $\mathbf{y}$ ) at the end of a DNN for multi-learning [13]. The output-gradient Jacobian is

$$\mathbf{J}_l^{(\mathcal{G})}(\mathbf{y}) = \frac{\partial \mathbf{g}_l(\mathbf{y})}{\partial \mathbf{y}} = \frac{\partial}{\partial \mathbf{y}} \left( \frac{\partial \ell(\mathbf{y}, \boldsymbol{\theta}_l)}{\partial \boldsymbol{\theta}_l} \right) \quad (9)$$

where  $\mathbf{g}_l(\cdot)$  represents the function that produces layer  $l$ ’s gradients  $\mathbf{G}_l \in \mathbb{R}^{N_l \times N_{l-1}}$  with true output  $\mathbf{y}$ . Besides,  $\ell(\cdot)$  is the loss function over  $\mathbf{y}$  and  $\boldsymbol{\theta}$  (parameters of the complete model), so  $\mathbf{g}_l(\cdot)$  can be regarded as the partial derivative of  $\ell(\cdot)$  *w.r.t.* layer  $l$ ’s parameters  $\boldsymbol{\theta}_l$  (*i.e.* backward propagation).

Because Jacobians are compared across layers, the magnitude and size of the layer’s parameters can also have an impact on the comparison results. More specifically, in [47] and [46], the Jacobian matrix is computed for the model outputs produced with the softmax function; so the outputs’ maximum value is bounded and the size is fixed for the same task (*i.e.* same number of classes). However, layers in one model have different numbers of neurons and can use unbounded activation functions such as the Rectifier Linear Unit (ReLU).

Therefore, we first bound the Jacobian matrix  $\mathbf{J}_l^{(\mathcal{G})}(\mathbf{y})$  with the range in gradients  $\mathbf{G}_l$  for layer  $l$ , which indicates the magnitude of Jacobian *w.r.t.* its original

value in gradients. Then we compute the norm of the Jacobian matrix similar to [47]. We use three standard norms including the Frobenius norm (refers as  $F$ -norm) for matrices and the 1-norm and the  $\infty$ -norm for vectors in order to capture adversaries with different capabilities. This is similar to the adversarial example [52, 54], where the  $p$ -norm reflects how the adversary measures distance between two data samples (*e.g.* 1-norm considers all dimensions of the data sample, and  $\infty$ -norm focuses on one dimension). After that, we normalize the *norm of Jacobian* with  $\mathbf{G}_l$ ’s size. Thus, given  $K$  data samples, we compute the bounded Jacobian with  $p$ -norm (referred to as ‘Jacobian  $p$ -norm’ hereinafter) averaged over the data samples as the privacy risk,

$$\frac{1}{K\psi_l} \sum_{k=1}^K \left\| \frac{\mathbf{J}_l^{(\mathcal{G})}(\mathbf{y}_k)}{\text{range}(\mathbf{g}_l(\mathbf{y}_k))} \right\|_p \quad (10)$$

where  $\text{range}(\cdot)$  returns the range of values in one vector (*i.e.*  $\max(\cdot) - \min(\cdot)$ ), and  $p = F, 1, \text{ or } \infty$ ,  $\psi_l$  is the normalization factor based on the size of the Jacobian matrix of layer  $l$  under each  $p$ .  $\psi_l = \sqrt{N_l \times N_{l-1}}$ ,  $N_l \times N_{l-1}$ , 1 for  $p = F, 1, \infty$ , respectively, used to balance the dimension differences of layers. We introduce  $\psi_l$  because the considered latent private information leakage [13] happens when the adversary concludes a binary inference (*i.e.* with/without the property); thus the final Jacobian norm should be reflected in one point (*i.e.* normalized by the layer size under each  $p$ ).

## 5 Empirical Setup

Next, we apply and validate the proposed metrics on several DNNs widely used in real-world applications. We first explain our experimental evaluation setup, which later has been used for the empirical layer-wise characterization and validation of the predictive ability of the proposed metrics.

**Goals and validity.** Our first goal is to apply the proposed metrics,  $\mathcal{V}$ -information and sensitivity, to characterize latent information privacy on the considered DNNs. The results of this characterization are presented in Section 6.1. Our second goal is to establish the validity of the privacy measurements. While our analysis is grounded in mathematical foundations we need an external or established approach to validate its results. We leverage the fact that the adversary’s success can be an indicator of privacy risks and commonly used in previous research [17, 19, 55, 56]; intuitively, if an adversary has access to information of higher risk this should



yield her better attack results. Therefore, to validate our proposed privacy metrics,  $\mathcal{V}$ -information and sensitivity, for each of the layers of a model, we compare them with the *PIA adversary's AUC* (*i.e.* area under the curve) score, which is the most common evaluation method for PIAs' success [13, 57], when they have access only to that layer. The results of PIAs validating the metrics are presented and discussed in Section 6.2 and 6.3. In addition, parameter settings of metrics such as the *chosen attack model* in  $\mathcal{V}$ -information and *norms* in sensitivity analysis may influence the evaluation results, so they are also measured together with validations.

**Models.** For our characterization and validation of the layer-wise privacy risk, we first use two DNN architectures, *variational AlexNet* and *VGG11Net* (similar to the target models in [13]). Both consist of several convolutional (Conv) layers as the earlier layer followed by several fully connected (FC) layers as the latter layers. This type of architecture is widely used because of its good performance; Conv layers capture features of the input data from low to high levels and then following FC layers process classification on them. Specifically, our AlexNet has three Conv layers with 16, 32, 64 filters of  $3 \times 3$  size (and each has a max-pooling with a size of (2, 2) after), followed by two FC layers with 256 and  $d_y$  neurons (where  $d_y$  is the output size or the number of classes). VGG11Net has eight Conv layers with 16, 16, 16, 16, 32, 32, 64, 64 filters of  $3 \times 3$  size (each of the last three has a max-pooling with a size of (2, 2) after), followed by three FC layers with 256, 128,  $d_y$  neurons, respectively. In addition, we include another fully connected network (FCNet) which has nine FC layers. All these FC layers have 32 neurons except the output (last) layer. The FCNet architecture has been used in previous research [31, 32]; by evaluating FCNet we aim to investigate the privacy risk when only FC layers are presented and when layers have the same size but different locations among the model. All three DNNs use ReLU activation functions for all layers (except the output layer).

**Datasets.** The three models described above are trained on three datasets with attributes, including Labeled Faces in the Wild (LFW) [58], Large-scale CelebFaces Attributes (CelebA) [59], and Public Figures Face Database (PubFig) [60]. LFW contains 13233 face images cropped and resized to  $62 \times 47$  RGB. All images are labeled with attributes such as gender, race, age, hair color, etc. CelebA contains more than 200k face images of celebrities with 40 attribute annotations such as gender, hair color, eyeglasses, etc. We use a subset

of the cropped version (*i.e.* 15000 images) and resize images to  $64 \times 64$  RGB. We also use a cropped version ( $100 \times 100$  RGB) of PubFig which contains 8300 facial images made up of 100 images for each of 83 persons [61]. All images are marked with 73 attributes (*e.g.* gender, race, etc).

**Setup.** We conduct our experiments on a cluster with multiple nodes where each has 4 Intel(R) Xeon(R) E5-2620 CPUs (2.00GHz), an NVIDIA RTX 6000 GPU (24GB), and 24GB DDR4 RAM. Deep learning framework Pytorch v1.4.0 is used for privacy measurements, and Theano v1.0 is used for PIAs.

We also follow the FL setting in the previous work [13] for comparing the privacy measurements with PIA results. Specifically, we conduct the learning process using FedSGD as the optimization algorithm. The learning rate is set as 0.01 without momentum. The batch size is 32. The training datasets above are partitioned as two parts to simulate two clients (more clients are similar in [13]). One client among them is assumed as the adversary. The adversary first participates in the training with others for several communication rounds (*e.g.* 100 rounds) then starts to save snapshots of the global model for conduct PIAs later. We also compute  $\mathcal{V}$ -information and sensitivity after the same number of communication rounds when measuring privacy.

## 6 Empirical Characterization and Validation

In this section, we present the results of measuring the privacy risk of layer-wise gradient sharing based on our proposed metrics, with respect to the PIA adversary's success rate, presented by AUC scores when given access to the target layer.

### 6.1 Layer-wise privacy characterization

The  $\mathcal{V}$ -information and sensitivity are measured on each layer of three models AlexNet, VGG11Net, and FCNet trained on three datasets LFW, CelebA, and PubFig, respectively. For the three datasets, the main task of FL is to learn 'Gender', 'Glasses', and 'Gender', respectively, and the test accuracy using FedSGD reaches 99%, 99%, 94% for LFW, 87%, 82%, 84% for CelebA, and 97%, 98%, 92% for PubFig.

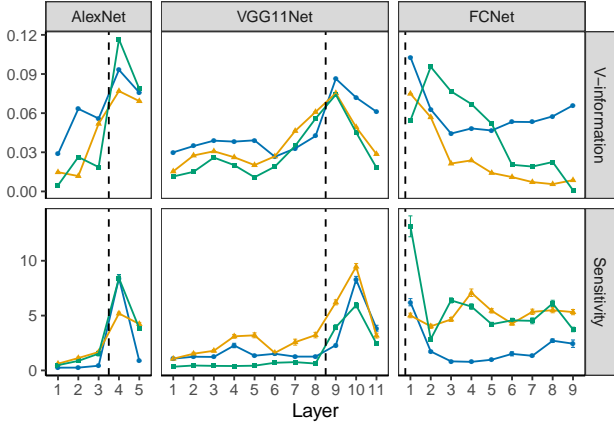


**Fig. 2.** Results of privacy measurements (*i.e.*  $\mathcal{V}$ -information and sensitivity) on each layer of AlexNet, VGG11Net, and FCNet, based on LFW (—), CelebA (—), PubFig (—) dataset. Dashed lines (—) refer to the connection from a Conv layer to a FC layer (*i.e.* all layers before it are Conv layers, and all layers after it are FC layers). Note that the sensitivity here is Jacobian  $F$ -norm. Each trail runs 20 times, and error bars are 95% confidence interval (CI) (some are too small to show).

We first only present Jacobian  $F$ -norm results for sensitivity (see the latter section for other norms). As shown in Figure 2 and Figure 3, in general, both  $\mathcal{V}$ -information and sensitivity predict the most vulnerable layer as the first FC layer. More specifically, they both have a similar pattern, showing that for these three models, the 4<sup>th</sup>, 9<sup>th</sup>/10<sup>th</sup>, and 1<sup>st</sup> layer have the highest privacy risk respectively. For AlexNet, the layer with the highest risk locates just after the last Conv layer (*i.e.* connecting to the first FC layer). This pattern is the same in the  $\mathcal{V}$ -information results of VGG11Net, but sensitivity indicates that the most sensitive layer is the 10<sup>th</sup> layer which differs from the prediction of  $\mathcal{V}$ -information (*i.e.* the 9<sup>th</sup> layer). One possible reason for this difference is that we compute the sensitivity *w.r.t.* outputs ( $\mathbf{y}$ ) instead of property ( $\mathbf{p}$ ), so it may then move towards the last output layer.

## 6.2 Validation on the particular property

To verify the above privacy characterization, we perform layer-wise PIAs using individual layer’s gradients (see Figure 3 for results). It shows that AUC scores have similar patterns with the prediction of both  $\mathcal{V}$ -information and sensitivity; *i.e.* the first FC layers have the highest private risk in terms of property information. We further conduct a Pearson correlation analysis (Table 1) to examine their relationship strength. The results in-

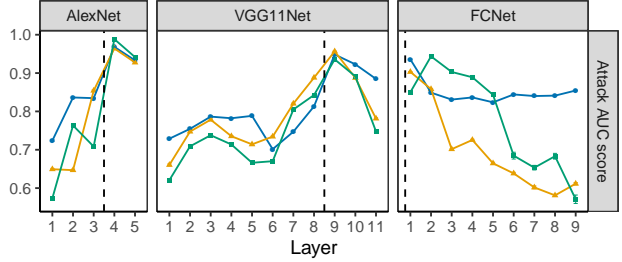


**Fig. 3.** AUC scores of property inference attacks on each layer’s gradients of AlexNet, VGG11Net, and FCNet based on LFW (—), CelebA (—), and PubFig (—). The property inference attack aims at ‘race: Black’, ‘gender: Female’, and ‘race: Black’, respectively. Dashed lines (—) refer to the connection from a Conv layer to a FC layer. Each trail run 20 times, and error bars are 95% CI (some are too small to show).

**Table 1.** Pearson correlation coefficient between prediction values (of  $\mathcal{V}$ -information and sensitivity) and attack AUC.

Model	$\mathcal{V}$ -information			Sensitivity		
	t	R	p-value	t	R	p-value
AlexNet	12.20	0.959	<0.001	3.60	0.707	0.003
VGG11Net	17.35	0.952	<0.001	5.25	0.686	<0.001
FCNet	18.41	0.965	<0.001	-0.73	-0.144	0.472
All	26.21	0.951	<0.001	2.73	0.304	0.008

dicates that  $\mathcal{V}$ -information has a very strong correlation with AUC scores for all models (with a correlation coefficient  $R > 0.95$  and significance  $p$ -value < 0.001), while sensitivity has a moderate or strong relationship with AUC scores for only AlexNet and VGG11Net. Although sensitivity suggests the first layers of FCNet are more sensitive, it has no correlation with AUC scores. This may be caused by the difference of learning patterns between FCNet and network with Conv layers—Conv layers in the latter one break input into common features ready for classifying by latter FC layers, but the former one that all layers are FC process all features together. However, in practice, almost all commonly used models follow the architecture similar to AlexNet and VGG11Net (*e.g.* Conv layers + FC layers). Thus, sensitivity is useful in characterizing layer-wise privacy for most applications. It is also worth noting that sensitivity may work better as a common privacy indicator independent from a particular PIA, because the calculation of sensitivity is independent of specific properties and attack methods.

**$\mathcal{V}$ -information’s attack model as a DNN.** Here we also build a DNN as the PIA model and test the  $\mathcal{V}$ -information and its AUC scores. A softmax function is needed at the end of the model, as claimed in [38], in

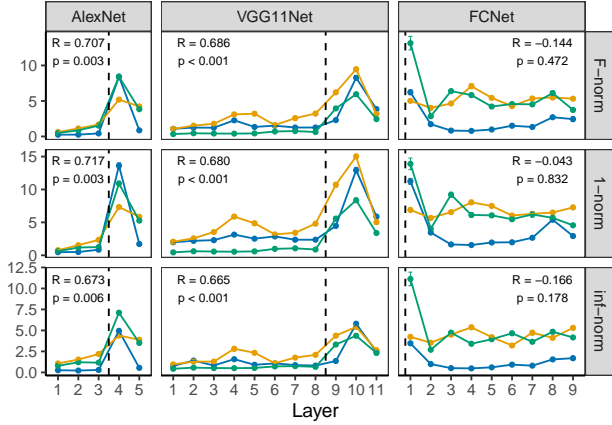


**Fig. 4.** Sensitivity measured with different Jacobian  $p$ -norm ( $p = F, 1$ , or  $\infty$ ) of each layer’s gradients of AlexNet, VGG11Net, and FCNet based on LFW (—), CelebA (—), and PubFig (—). Dashed lines (—) refer to the connection from a Conv layer to a FC layer. The  $R$  and  $p$ -value refer to correlation coefficient and significance in Pearson correlation analysis between the norm and attack AUC scores. Each trail runs 20 times, and error bars are 95% CI (some are too small to show).

order to output distribution density over ground truths. A typical DNN model usually has it for computing loss. In Figure 5, the results show that a PIA using DNNs follows the same pattern; the target model’s layers after the connection between the last Conv layer and the first FC layer have the highest AUC score. They also have the highest  $\mathcal{V}$ -information indicating that these layers have the highest privacy risk. It is also found that RF outperforms DNNs as the attack model; thus, when computing  $\mathcal{V}$ -information, setting predictive family to RF, which is a more powerful one, can give us better prediction in terms of private information contained in layers’ gradients.

**Sensitivity with  $p$ -norm and layers’ sizes.** As the layer size and the norm can influence sensitivity analysis results, here we present the other Jacobian  $p$ -norm (1, or  $\infty$ ) in addition to Jacobian  $F$ -norm. The results (see Figure 4) indicate that all tend to have similar patterns and the more sensitive part is after the connection line. For these two Conv networks (*i.e.* AlexNet and VGG11Net), the correlation coefficient ( $R$ ) keep at the moderate or strong level with  $p$ -value  $< 0.006$ . The sensitivity comparison among layers gives the same results no matter how the distance between two Jacobian matrices is computed by the different norms.

It is worth noting that all norms are divided by a factor of the matrix’s size (see Equation 10) which we first aimed at the comparison across layers’ Jacobians

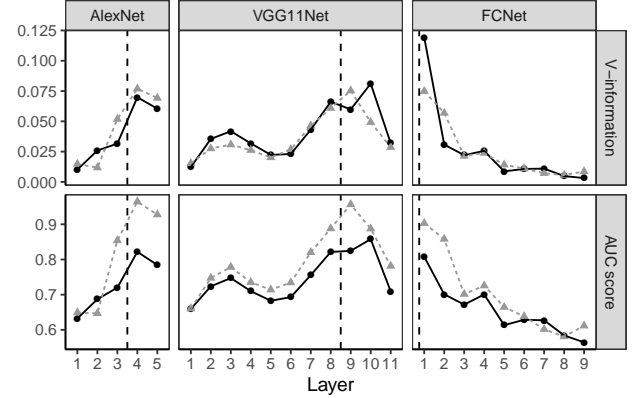


**Fig. 5.** Property inference attack AUC score and corresponding  $\mathcal{V}$ -information when using deep learning models as the attack model (—). The results of using random forest (---) is shown for comparison. Black dashed lines (—) refer to the connection from a Conv layer to a FC layer. Each trail runs 20 times, and error bars (95% CI) are too small to show.

with different sizes; however, it also partly reflects the sensitivity per unit (neuron). Specifically, the difference among layers can be driven by both the layer’s location in the model and the layer’s size. Several layers (*e.g.* the last Conv layer or the first FC layers) may contain more neurons, so their gradients have a higher dimension and richer information which benefit the attacker with an improvement of PIA performance.

In addition to that, a latter FC layer seems to contain more property information (that is easier to be captured by PIA model [13]) than an earlier Conv layer with the same or even larger dimension. For example, in Figure 7 (PIAs on other properties) the first several layers are Conv layers with a size of 2304 (the number of filters is 16). their sizes reduce to 256 by max-pooling function (in PIAs [13]) before inputting to the PIA model, while the 11<sup>th</sup> layer is also a FC layer with size 256. From the results, we observe that the 11<sup>th</sup> layer tends to have a higher AUC score, especially regarding the property of age and gender. Therefore, the latter layer still is considered as being more sensitive per unit neuron compared to former Conv layers. As an example, we randomly pick gradients of 48 neurons from each layer and then conduct PIA on them. Results show layers around the connection between Conv layers and FC layers) still results in higher AUC scores with a similar pattern of complete gradients (see Figure 6). This may be captured by the normalization factor (*i.e.* size of the Jacobian matrix) in sensitivity, which is meaningful considering the limited protection resources in which we can only preserve a certain number of neurons.

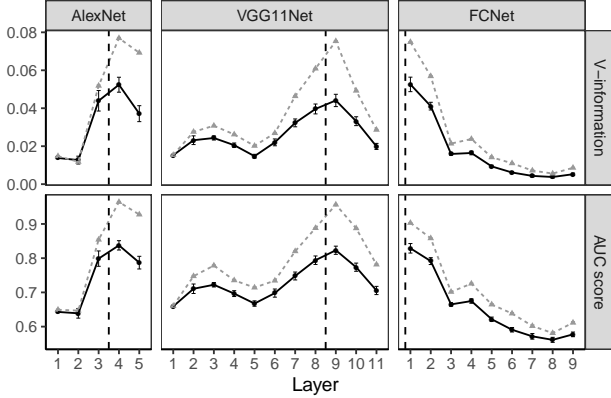


**Fig. 6.** Property inference attack AUC score and corresponding  $\mathcal{V}$ -information when only 48 random gradients (—) are used. Results of attacking using all gradients are also presented in grey dashed lines (---). Vertical dashed lines (- -) indicate the connection from a Conv layer to a FC layer. Each trail runs 20 times, and error bars are 95% CI.

### 6.3 Validation on multiple properties

**Validation on attacks of other properties.** In Figure 3 we show the PIA result on one property (to infer the race is black or not) to verify  $\mathcal{V}$ -information and sensitivity. Both succeed in predicting the DNN’s sensitive part but the former one outperforms the latter one. However, we expect that the performance of  $\mathcal{V}$ -information computed on one specific property to drop in terms of other latent information (*e.g.* another property), while sensitivity can still keep the same level of performance. Figure 7 illustrates the cases where the main task of FL is the classification of glasses, and the PIA aims to infer properties of *age*, *gender*, and *hair*. We observe similar patterns for PIAs on all properties: the 9<sup>th</sup> layer, *i.e.* the first FC layer in VGG11Net, leaks the largest amount of property information. However, as expected, we observe a decreasing prediction capability of  $\mathcal{V}$ -information on the other property, and an increased capability of sensitivity. Consider for example the property ‘Gender’ (middle figure). The correlation coefficient ( $R$ ) of  $\mathcal{V}$ -information drops 0.357 from 0.952 (in Table 1) to 0.595 (moderate correlation), and that of sensitivity increases 0.136 from 0.686 to 0.822 (strong correlation). The results verify the applicability of sensitivity as the layer-wise privacy indicator.

**Comparison between  $\mathcal{V}$ -information and sensitivity.** The extremely high prediction accuracy of  $\mathcal{V}$ -information comes at a price of transferability since it is computed using not only one specific (*i.e.* the best) attack model in the adversaries’ predictive family which

in reality may not be known by the defender but also one specific attack target (*e.g.* property). When the adversary changes its attack model without the defenders’ knowledge or the attack target,  $\mathcal{V}$ -information may have a much weaker capability of prediction.

By contrast, sensitivity is independent of the attack model because it is directly computed based on the Jacobian matrix of the gradients *w.r.t.* model outputs. It can be seen as a more universal way of measuring property privacy risk (even if it can contain more biases). One reason for the slight deviation for predicting the most sensitive layer when using sensitivity may come from the fact that we compute the gradients for the model outputs. We expect better prediction results could be achieved if the Jacobian matrix would be computed *w.r.t.* property, *i.e.*  $\mathbf{J}_l^{(G)}(\mathbf{p})$ . However, this may still lead to less transferability since it is aimed at one particular latent information.

Here we remark that one explanation for similar AUC patterns in Figure 7 is that all these properties, *i.e.* the high-level features, tend to be best captured in a similar part—around the connection between the first FC layers and the last Conv layers. Therefore, defenses on different properties can be similar in terms of the set of layers, although the PIA results slightly differ in properties. That is, one benefit of protecting (the same) layers is that one can guarantee potential information leakage for multiple properties at once.

**Sensitivity on different tasks.** The above analyses study which layers are most likely to leak information while fixing the classification (main) task. Here we compare the sensitivity (using the Jacobian  $F$ -norm) across main tasks, *i.e.* when other attributes (or properties) are set as the classification tasks. This aims to explore the influence of the particular task on the performance of the sensitivity metric, as well as to understand if the localization of sensitive information changes depending on the task. We evaluate the results on two DNNs: AlexNet and VGG11Net, and train them on LFW with five attributes as the classification task. The test accuracy using FedSGD reaches 99%, 99% for ‘Gender’ (2 classes), 80%, 89% for ‘Glasses’ (3 classes), 76%, 75% for ‘Race’ (3 glasses), 52%, 49% for ‘Hair’ (4 classes), and 43%, 33% for Age (5 classes) on these two models, respectively.

Similar to the above analyses, sensitivity with the Jacobian  $F$ -norm is measured layer-wisely. However, sensitivity *w.r.t.* different tasks has a large range even on the same layer of one model. This may be caused by the difference in the training process of classification

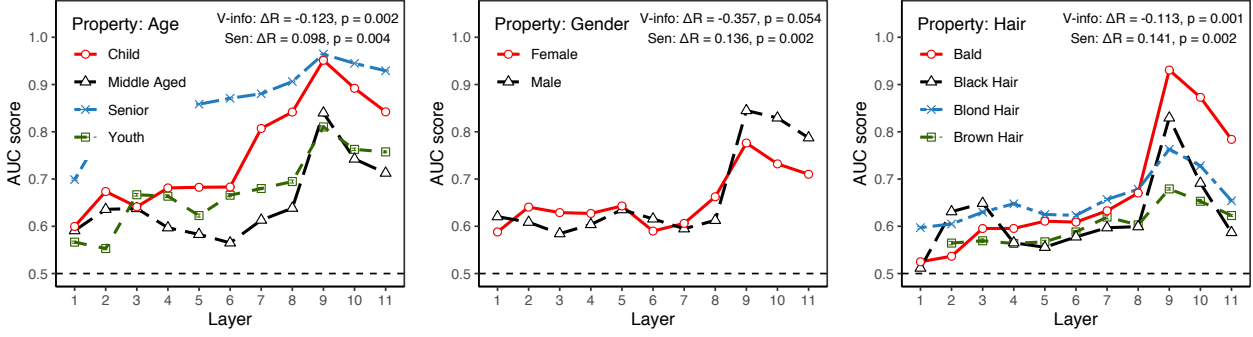


**Fig. 7.** AUC scores of property inference attacks aiming at different properties of Age, Gender, and Hair. Attacks are on each layer of VGG11Net trained on LFW with Glasses as the main task. Pearson correlations between the AUC score and privacy metric ( $\mathcal{V}$ -information and sensitivity) are given at the top right corner.  $\Delta R$  refers to the changes of correlation coefficient compared to that in Figure 2.  $p$ -value refers to significance. Each trail runs 20 times, and error bars (95% CI) are too small to show.

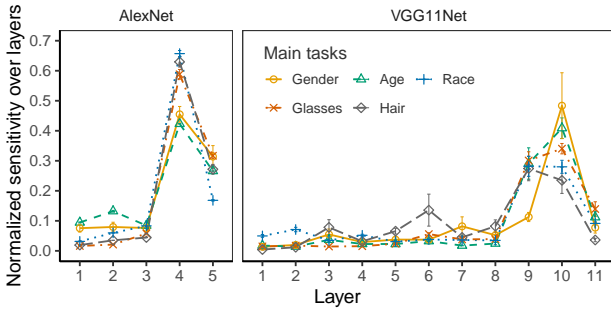


**Fig. 8.** Normalized sensitivity over all layers of one model. The sensitivity is measured with Jacobian  $F$ -norm of each layer’s gradients of AlexNet and VGG11Net, both convolutional networks, trained on LFW. Each trail runs 20 times, and error bars are 95% CI (some are too small to show).

tasks; the training may learn ‘faster’ on one task than another and the gradient also changes ‘faster’. Therefore, we further normalize sensitivity over all layers of one model (*i.e.* to make the summation be 1) in order to make them comparable across different main tasks. Figure 8 shows that no matter what the main classification task is, the first FC layers after the last Conv layer (*i.e.* layer  $4^{th}$  in AlexNet and layer  $9^{th}$  or  $10^{th}$  in VGG11Net) always have the highest (normalized) sensitivity. Moreover, we observe that, with AlexNet, ‘Gender’ and ‘Age’ have lower sensitivity than the others in layer  $4^{th}$ ; with VGG11Net, they have higher sensitivity than the others in layer  $10^{th}$ , but ‘Gender’ has the lowest sensitivity in layer  $9^{th}$ . It is shown that different attributes have different distributions of sensitivity among layers and models.

To gain a better understanding into which models and layers could leak which *type* of information, we classify these attributes as lower- or higher-level latent in-

formation based on the intuition of how one attribute relates to the original face image. Specifically, if learning one attribute involves the understanding of the entire image, we regard it as higher-level latent information (*i.e.* gender and age). When learning it involves the understanding of only a part of the image, we regard it as lower-level latent information (*i.e.* glasses and hair). Then, for VGG11Net, although tasks have similar sensitivity on many layers, we can still find that for layer  $10^{th}$ , higher-level features ‘Gender’ and ‘Age’ have higher sensitivity than the others. ‘Gender’ also has the lowest sensitivity in layer  $9^{th}$ . Meanwhile, lower-level feature ‘Hair’ has the lowest sensitivity in layers  $10^{th}$  and  $11^{th}$  but a higher one in many former layers. Therefore, it is shown that in general higher-level latent information has the tendency to be present more in the last layers. However, for AlexNet, ‘Gender’ and ‘Age’ instead have the lowest sensitivity in layer  $4^{th}$ . This may be due to differences in the DNN architectures, as the last three layers of VGG11Net are FC while only the last two layers of AlexNet are FC; ‘Gender’ and ‘Age’ still have a high sensitivity in AlexNet’s layer  $5^{th}$ . Our analysis shows the potential of using sensitivity metrics to precisely understand where and what type of information is stored.

## 7 Discussion

**On  $\mathcal{V}$ -information as a privacy metric.** Although one can use the AUC of PIAs to directly measure which layers are more sensitive; there is no theoretical support for this. Moreover, the type and implementation of potential attacks are not restricted to PIA and its

specific implementation, thus one can argue that the results of a specific attack may not be a reliable measure when considering another attack (even for a small change in the adversary model). Under the assumption that  $\mathcal{V}$  is a predictive family (see Definition 1), the empirical  $\mathcal{V}$ -information gives a theoretically grounded way of measuring the ‘usable information’ that is contained in the gradients for performing the attack. It can thus be used as a predictor for how well a subset of potential attacks will work on the shared gradients. Furthermore, by its definition through the *infimum* over the models in the predictive family, we only need to find the ‘best’ attack model, in order to measure the success of a general class of attacks. For example, we can define the predictive family as one specific DNN architecture and by training it with SGD or similar approaches, we achieve an (almost) optimal model whose  $\mathcal{V}$ -information represents the attack success of the complete predictive family [38]. We can also define the predictive family as all the tested attacks (*e.g.* including RF, DNN, or any other machine learning models under the technical assumption that this family satisfies Definition 1) and then choose the best one that outperforms the others. In this case,  $\mathcal{V}$ -information can be used as a theoretically grounded indicator of privacy leakage.

**On sensitivity as a privacy metric.** Sensitivity analysis can overcome the requirement of defining a predictive family. The sensitivity can measure the generalization and robustness of DNN models [47]. Following the same concept, our underlying idea is that by measuring how much a change in the input (*e.g.* by the addition of noises) leads to a change in the model output. If this is small, the model is less sensitive, *i.e.* more robust, to changes in the input. Using sensitivity as a privacy metric follows the idea that the ability of gradients to leak private information is related to how distinguishable the gradient is *w.r.t.* one certain property in data. More specifically, if changing the data by removing samples with a certain property leads to no change in the gradients, these gradients are unlikely to leak information about this property. For example, if two similar face images from a training set which only differ from each other in the race property (*e.g.* White and Black) result in a huge difference in the updated model parameters/gradients, these parameters/gradients can be used to predict the race property (same interpretation for the binary classifier PIA in [13]). Hence, although the sensitivity does not directly measure the sensitive information, it measures fine-grained changes caused by one sample data. Therefore, as we saw, it is a good indicator

of the attacker’s success rate in discovering a sensitive property. More importantly, the sensitivity is independent of both the particular attack model and the targeted private information, which makes it a more general metric for localizing and understanding latent information leakages. Furthermore, we discuss the approximate relationship between sensitivity and  $\mathcal{V}$ -information based on Taylor approximation in Appendix 9.4.

**On the difficulty of protecting latent information.** To defend against PIAs is difficult; for example, an adversary with access to a single least-sensitive layer (from the privacy metric evaluation), already results in an AUC of around 0.6 for the attack success rate (see Figure 7 as an example). One possible reason for the difficulty in preventing property information leakage is that it concerns very high-level latent information in gradients. Indeed, popular defenses such as adding noise as in DP fail to prevent this attack [13], because property information in gradients is of large-level DP granularity where the small-level granularity protection of DP cannot guarantee its privacy [50]. For clarification, we can consider the privacy leakage from the layer’s intermediate representation,  $T$ . Because of the direct mapping from original data  $X$  to  $T$  (see Section 4.1), an attacker can get pixel-level recovery of one specific image. Then, a pixel-level DP with small noise additions (Gaussian noise with  $\sigma = 10^{-3} \sim 10^{-2}$ ) manages to defend against such an adversarial recovery [9]. However, if an attacker aims at inferring a property of  $X$ , it could be that several parts of the image contain correlated information about this property, so the DP needs to be defined at larger granularity. Consequently, more noises are required to guarantee privacy under this granularity which may, in turn, ruin the model training process.

**On the most sensitive layer.** The location of the most sensitive layer in a model can change depending on the type of information. More specifically, the first layer contains the most sensitive information of the original input [9, 10] (see also Appendix 9.2), and the last layer contains the most membership information (*i.e.* presence in the training phase) of the input [12, 20, 56]. Regarding property information, we found that the first FC layers (usually just after the last Conv layer) are the most sensitive layer. One explanation is that property information between the original information,  $X$ , and output information,  $Y$ , is best captured in a middle layer. In addition, the property is a high-level feature; the FC layer classifies the feature maps from the previous Conv layers, and it can contain distinguishable high-level latent information such as the property. Similarly,

the last Conv layer is likely to have more property information than previous Conv layers, because initial Conv layers learn more general information (*e.g.* ambient colors or edge in images), while latter Conv layers focus on high-level latent information (*e.g.* face identity) [29, 30]. We note that there are still differences among properties as shown in Figure 7 explaining where certain properties are most likely to be captured. Besides, we also find the tendency that higher-level properties can be more sensitive in the latter layers while lower-level properties are more sensitive in former layers, which deserves detailed analysis in future work.

**On the impact of aggregation: FedSGD vs. FedAvg.** As the attack performance is influenced by the level of aggregation [13], the privacy risk on layers with different aggregation in FL can also change. The original PIA we tested was based on FedSGD, in which the model will be updated after each training step. In this case, we identify the last FC layers and even the last Conv layer to be the most sensitive part. When the aggregation is slightly stronger, for example, multiple clients participate in the FedSGD, gradients leak less information about a single client, but the attack still manages to reveal some property information [13]. For FedAvg that involves much more aggregation, there are no empirical results verifying the effectiveness of PIAs. However, we argue that it depends on the complexity of the contained information about the clients’ dataset. Even if shared gradients are updated based on the complete dataset for multiple epochs, it is possible to conduct PIAs on these gradients when this dataset contains clear property information (*e.g.* all images contain a black or white face). In this case, we believe the PIA will still be successful. When aggregated gradients contain too complex information to successfully perform PIAs, another potential attack is MIA [12]. In this case, we expect that the most sensitive part of the model moves to the last layer [56]. Furthermore, a recent FL design, FedMA [22], trains the model in a layer-wise manner and achieves a higher model growth rate while requiring a smaller number of communication rounds than state-of-the-art FL approaches. It performs local training with more epochs (*e.g.* 100 number of epochs), so the privacy risk may further reduce.

**On defending against latent information leakage.** Our layer-wise characterization highlights opportunities for designing defenses that are flexible and practical at the layer-level. For example, FHE-based approaches fully respect the model privacy but it leads to extremely high runtime overhead. Our analysis could help by pro-

viding a solution utilizing FHE only on the sensitive part of the model during training. In addition, given the resource constraints on edge devices, Trusted Execution Environment (TEE)-based approaches with model partitioning also become a promising approach. Specifically, during FL, one can deploy and run the most sensitive layers (*e.g.* the last Conv layer and the first FC layer) inside the TEE using model partitioned execution technique across trusted and untrusted environment similar to [56]. Our layer-wise measurement may also benefit this FL design by the ability to protect the most sensitive layers in the TEE. We also expect that there may exist one way to layer-wisely federated training a model (similar to FedMA), *e.g.* in TEEs, which could further reduce the privacy risk by exposing only one layer instead of the complete model.

Furthermore, there are privacy-preserving techniques proposing to add noise to gradients (*i.e.* DP), share fewer gradients, or use dimensionality reduction and regularization (*e.g.* Dropout). However, none of them can handle the PIAs without compromising model utility [13]. For example, sharing fewer gradients guarantees model privacy aims to limit the total number of gradients the adversary could access. However, as it is evident from [13] and in Figure 6, sharing fewer gradients does not fully guarantee privacy. Sharing 10% of the gradients still leads to 0.84 attack AUC, while sharing all gradients has 0.93 AUC. The reason for its low privacy preservation performance is that gradients are randomly dropped, hence it is possible that some highly sensitive gradients still remain to share.

## 8 Conclusion

In this work, we proposed two mathematically-motivated metrics and took a significant step forward in the understanding of the severe and open question—latent information leakage, *e.g.* a client’s private property, in federated learning. We adopted  $\mathcal{V}$ -information as a notion of measuring the usable information contained in the gradients of each layer of a DNN. We empirically validated the ability of  $\mathcal{V}$ -information to quantify the success of a property inference adversary with access to specific layers of DNNs. We also proposed and validated a metric based on sensitivity analysis which allows us to localize property information *independent of* the adversary model and the target property. For the first time, we found that in the most common networks (*i.e.* convolutional neural networks), the first fully connected

layer that comes after the last convolutional layer is the most sensitive layer *w.r.t.* high-level latent information such as the gender or race. Moreover, we showed that higher-level and lower-level properties are more likely to be revealed via the latter layers and former layers in DNNs, respectively. Our layer-wise characterization provides a better understanding of the memorization of data in neural networks and reveals opportunities to design flexible layer-level defenses for a better trade-off between privacy guarantees and cost.

## References

- [1] B. McMahan, E. Moore, D. Ramage, S. Hampson, and B. A. y Arcas, "Communication-efficient learning of deep networks from decentralized data," in *Artificial Intelligence and Statistics*, 2017, pp. 1273–1282.
- [2] P. Kairouz, H. B. McMahan, B. Avent, A. Bellet, M. Ben- nis, A. N. Bhagoji, K. Bonawitz, Z. Charles, G. Cormode, R. Cummings *et al.*, "Advances and open problems in federated learning," *arXiv preprint arXiv:1912.04977*, 2019.
- [3] K. Bonawitz, V. Ivanov, B. Kreuter, A. Marcedone, H. B. McMahan, S. Patel, D. Ramage, A. Segal, and K. Seth, "Practical secure aggregation for privacy-preserving machine learning," in *Proceedings of the 2017 ACM SIGSAC Conference on Computer and Communications Security*. ACM, 2017, pp. 1175–1191.
- [4] T. Yang, G. Andrew, H. Eichner, H. Sun, W. Li, N. Kong, D. Ramage, and F. Beaufays, "Applied federated learning: Improving google keyboard query suggestions," *arXiv preprint arXiv:1812.02903*, 2018.
- [5] A. Hard, K. Rao, R. Mathews, S. Ramaswamy, F. Beaufays, S. Augenstein, H. Eichner, C. Kiddon, and D. Ramage, "Federated learning for mobile keyboard prediction," *arXiv preprint arXiv:1811.03604*, 2018.
- [6] K. Bonawitz, H. Eichner, W. Grieskamp, D. Huba, A. In-german, V. Ivanov, C. Kiddon, J. Konečný, S. Mazzocchi, H. B. McMahan *et al.*, "Towards federated learning at scale: System design," in *Twelve Conference on Machine Learning and Systems*, 2019.
- [7] M. Naseri, J. Hayes, and E. De Cristofaro, "Toward robustness and privacy in federated learning: Experimenting with local and central differential privacy," *arXiv preprint arXiv:2009.03561*, 2020.
- [8] B. Hitaj, G. Ateniese, and F. Perez-Cruz, "Deep models under the gan: information leakage from collaborative deep learning," in *Proceedings of the 2017 ACM SIGSAC Conference on Computer and Communications Security*. ACM, 2017, pp. 603–618.
- [9] L. Zhu, Z. Liu, and S. Han, "Deep leakage from gradients," in *Advances in Neural Information Processing Systems*, 2019, pp. 14 747–14 756.
- [10] J. Geiping, H. Bauermeister, H. Dröge, and M. Moeller, "In-verting gradients—how easy is it to break privacy in federated learning?" *arXiv preprint arXiv:2003.14053*, 2020.
- [11] Z. Wang, M. Song, Z. Zhang, Y. Song, Q. Wang, and H. Qi, "Beyond inferring class representatives: user-level privacy leakage from federated learning," in *IEEE INFO-COM 2019-IEEE Conference on Computer Communications*. IEEE, 2019, pp. 2512–2520.
- [12] M. Nasr, R. Shokri, and A. Houmansadr, "Comprehensive privacy analysis of deep learning: Passive and active white-box inference attacks against centralized and federated learning," in *2019 IEEE Symposium on Security and Privacy (SP)*. IEEE, 2019, pp. 739–753.
- [13] L. Melis, C. Song, E. De Cristofaro, and V. Shmatikov, "Exploiting unintended feature leakage in collaborative learning," in *2019 IEEE Symposium on Security and Privacy (SP)*. IEEE, 2019, pp. 691–706.
- [14] R. Shokri, M. Stronati, C. Song, and V. Shmatikov, "Membership inference attacks against machine learning models," in *2017 IEEE Symposium on Security and Privacy (SP)*. IEEE, 2017, pp. 3–18.
- [15] J. Hayes, L. Melis, G. Danezis, and E. De Cristofaro, "Logan: Membership inference attacks against generative models," *Proceedings on Privacy Enhancing Technologies*, vol. 2019, no. 1, pp. 133–152, 2019.
- [16] Y. Liu, S. Ma, Y. Aafer, W.-C. Lee, J. Zhai, W. Wang, and X. Zhang, "Trojanning attack on neural networks," in *Network and Distributed Systems Security (NDSS) Symposium 2018*, 2018.
- [17] W. Wei, L. Liu, M. Loper, K.-H. Chow, M. E. Gursoy, S. Truex, and Y. Wu, "A framework for evaluating gradient leakage attacks in federated learning," *arXiv preprint arXiv:2004.10397*, 2020.
- [18] B. Zhao, K. R. Mopuri, and H. Bilen, "idlg: improved deep leakage from gradients," *arXiv preprint arXiv:2001.02610*, 2020.
- [19] S. Yeom, I. Giacomelli, M. Fredrikson, and S. Jha, "Privacy risk in machine learning: Analyzing the connection to overfitting," in *2018 IEEE 31st Computer Security Foundations Symposium (CSF)*. IEEE, 2018, pp. 268–282.
- [20] A. Sablayrolles, M. Douze, C. Schmid, Y. Ollivier, and H. Jégou, "White-box vs black-box: Bayes optimal strategies for membership inference," in *International Conference on Machine Learning*, 2019, pp. 5558–5567.
- [21] Y. Aono, T. Hayashi, L. Wang, S. Moriai *et al.*, "Privacy-preserving deep learning via additively homomorphic encryption," *IEEE Transactions on Information Forensics and Security*, vol. 13, no. 5, pp. 1333–1345, 2017.
- [22] H. Wang, M. Yurochkin, Y. Sun, D. Papailiopoulos, and Y. Khazaeni, "Federated learning with matched averaging," in *International Conference on Learning Representations (ICLR)*, 2019.
- [23] Y. LeCun, Y. Bengio, and G. Hinton, "Deep learning," *nature*, vol. 521, no. 7553, pp. 436–444, 2015.
- [24] B. Neyshabur, S. Bhojanapalli, D. McAllester, and N. Srebro, "Exploring generalization in deep learning," in *Advances in Neural Information Processing Systems*, 2017, pp. 5947–5956.
- [25] Y. Kaya, S. Hong, and T. Dumitras, "Shallow-deep networks: Understanding and mitigating network overthinking," in *International Conference on Machine Learning*. PMLR, 2019, pp. 3301–3310.



- [26] J. Lee, S. S. Schoenholz, J. Pennington, B. Adlam, L. Xiao, R. Novak, and J. Sohl-Dickstein, "Finite versus infinite neural networks: an empirical study," *arXiv preprint arXiv:2007.15801*, 2020.
- [27] S. Arora, S. S. Du, W. Hu, Z. Li, R. R. Salakhutdinov, and R. Wang, "On exact computation with an infinitely wide neural net," in *Advances in Neural Information Processing Systems*, 2019, pp. 8141–8150.
- [28] A. Achille, G. Paolini, and S. Soatto, "Where is the information in a deep neural network?" *arXiv preprint arXiv:1905.12213*, 2019.
- [29] M. D. Zeiler and R. Fergus, "Visualizing and understanding convolutional networks," in *European conference on computer vision*. Springer, 2014, pp. 818–833.
- [30] A. Mahendran and A. Vedaldi, "Understanding deep image representations by inverting them," in *Proceedings of the IEEE conference on computer vision and pattern recognition*, 2015, pp. 5188–5196.
- [31] R. Shwartz-Ziv and N. Tishby, "Opening the black box of deep neural networks via information," *arXiv preprint arXiv:1703.00810*, 2017.
- [32] A. M. Saxe, Y. Bansal, J. Dapello, M. Advani, A. Kolchinsky, B. D. Tracey, and D. D. Cox, "On the information bottleneck theory of deep learning," *Journal of Statistical Mechanics: Theory and Experiment*, vol. 2019, no. 12, p. 124020, 2019.
- [33] Z. Goldfeld, E. Van Den Berg, K. Greenewald, I. Melnyk, N. Nguyen, B. Kingsbury, and Y. Polyanskiy, "Estimating information flow in deep neural networks," in *International Conference on Machine Learning*, 2019, pp. 2299–2308.
- [34] M. Abadi, A. Chu, I. Goodfellow, H. B. McMahan, I. Mironov, K. Talwar, and L. Zhang, "Deep learning with differential privacy," in *Proceedings of the 2016 ACM SIGSAC Conference on Computer and Communications Security*, 2016, pp. 308–318.
- [35] R. C. Geyer, T. Klein, and M. Nabi, "Differentially private federated learning: A client level perspective," *arXiv preprint arXiv:1712.07557*, 2017.
- [36] E. Shi, H. Chan, E. Rieffel, R. Chow, and D. Song, "Privacy-preserving aggregation of time-series data," in *Annual Network & Distributed System Security Symposium (NDSS)*. Citeseer, 2011.
- [37] C. E. Shannon, "A mathematical theory of communication," *Bell system technical journal*, vol. 27, no. 3, pp. 379–423, 1948.
- [38] Y. Xu, S. Zhao, J. Song, R. Stewart, and S. Ermon, "A theory of usable information under computational constraints," in *International Conference on Learning Representations (ICLR)*, 2020.
- [39] K. Simonyan and A. Zisserman, "Very deep convolutional networks for large-scale image recognition," *arXiv preprint arXiv:1409.1556*, 2014.
- [40] G. A. Kaissis, M. R. Makowski, D. Rückert, and R. F. Braren, "Secure, privacy-preserving and federated machine learning in medical imaging," *Nature Machine Intelligence*, pp. 1–7, 2020.
- [41] L. v. d. Maaten and G. Hinton, "Visualizing data using t-sne," *Journal of machine learning research*, vol. 9, no. Nov, pp. 2579–2605, 2008.
- [42] N. Tishby, F. C. Pereira, and W. Bialek, "The information bottleneck method," *arXiv preprint physics/0004057*, 2000.
- [43] Y. Bengio, A. Courville, and P. Vincent, "Representation learning: A review and new perspectives," *IEEE transactions on pattern analysis and machine intelligence*, vol. 35, no. 8, pp. 1798–1828, 2013.
- [44] D. McAllester and K. Stratos, "Formal limitations on the measurement of mutual information," in *International Conference on Artificial Intelligence and Statistics*, 2020, pp. 875–884.
- [45] J. Song and S. Ermon, "Understanding the limitations of variational mutual information estimators," in *International Conference on Learning Representations*, 2019.
- [46] J. Sokolić, R. Giryes, G. Sapiro, and M. R. Rodrigues, "Robust large margin deep neural networks," *IEEE Transactions on Signal Processing*, vol. 65, no. 16, pp. 4265–4280, 2017.
- [47] R. Novak, Y. Bahri, D. A. Abolafia, J. Pennington, and J. Sohl-Dickstein, "Sensitivity and generalization in neural networks: an empirical study," in *International Conference on Learning Representations (ICLR)*, 2018.
- [48] T. Zahavy, B. Kang, A. Sivak, J. Feng, H. Xu, and S. Mannor, "Ensemble robustness and generalization of stochastic deep learning algorithms," 2018.
- [49] G. W. Ding, K. Y. C. Lui, X. Jin, L. Wang, and R. Huang, "On the sensitivity of adversarial robustness to input data distributions," in *International Conference on Learning Representations*, 2018.
- [50] C. Dwork, A. Roth *et al.*, "The algorithmic foundations of differential privacy," *Foundations and Trends in Theoretical Computer Science*, vol. 9, no. 3–4, pp. 211–407, 2014.
- [51] F. McSherry and K. Talwar, "Mechanism design via differential privacy," in *48th Annual IEEE Symposium on Foundations of Computer Science (FOCS'07)*. IEEE, 2007, pp. 94–103.
- [52] M. Lecuyer, V. Atlidakis, R. Geambasu, D. Hsu, and S. Jana, "Certified robustness to adversarial examples with differential privacy," in *2019 IEEE Symposium on Security and Privacy (SP)*. IEEE, 2019, pp. 656–672.
- [53] Z. Gu, H. Huang, J. Zhang, D. Su, H. Jamjoom, A. Lamba, D. Pendarakis, and I. Molloy, "Yerbabuena: Securing deep learning inference data via enclave-based ternary model partitioning," *arXiv preprint arXiv:1807.00969*, 2018.
- [54] M. Cissé, P. Bojanowski, E. Grave, Y. Dauphin, and N. Usunier, "Parseval networks: Improving robustness to adversarial examples," in *International Conference on Machine Learning*, 2017.
- [55] B. Jayaraman and D. Evans, "Evaluating differentially private machine learning in practice," in *28th {USENIX} Security Symposium ({USENIX} Security 19)*, 2019, pp. 1895–1912.
- [56] F. Mo, A. S. Shamsabadi, K. Katevas, S. Demetriou, I. Leontiadis, A. Cavallaro, and H. Haddadi, "Darknetz: towards model privacy at the edge using trusted execution environments," in *Proceedings of the 18th International Conference on Mobile Systems, Applications, and Services*, 2020, pp. 161–174.
- [57] D. M. Powers, "Evaluation: From precision, recall and f-measure to roc, informedness, markedness & correlation," *Journal of Machine Learning Technologies*, vol. 2, no. 1, pp. 37–63, 201.

- [58] G. B. Huang, M. Mattar, T. Berg, and E. Learned-Miller, "Labeled faces in the wild: A database for studying face recognition in unconstrained environments," 2008.
- [59] Z. Liu, P. Luo, X. Wang, and X. Tang, "Deep learning face attributes in the wild," in *Proceedings of International Conference on Computer Vision (ICCV)*, December 2015.
- [60] N. Kumar, A. C. Berg, P. N. Belhumeur, and S. K. Nayar, "Attribute and simile classifiers for face verification," in *2009 IEEE 12th international conference on computer vision*. IEEE, 2009, pp. 365–372.
- [61] N. Pinto, Z. Stone, T. Zickler, and D. Cox, "Scaling up biologically-inspired computer vision: A case study in unconstrained face recognition on facebook," in *CVPR 2011 WORKSHOPS*. IEEE, 2011, pp. 35–42.
- [62] A. Kraskov, H. Stögbauer, and P. Grassberger, "Estimating mutual information," *Physical review E*, vol. 69, no. 6, p. 066138, 2004.
- [63] A. Kolchinsky, B. D. Tracey, and D. H. Wolpert, "Nonlinear information bottleneck," *Entropy*, vol. 21, no. 12, p. 1181, 2019.
- [64] M. I. Belghazi, A. Baratin, S. Rajeshwar, S. Ozair, Y. Bengio, A. Courville, and D. Hjelm, "Mutual information neural estimation," in *International Conference on Machine Learning*, 2018, pp. 531–540.
- [65] A. Elad, D. Haviv, Y. Blau, and T. Michaeli, "Direct validation of the information bottleneck principle for deep nets," in *Proceedings of the IEEE International Conference on Computer Vision Workshops*, 2019, pp. 0–0.
- [66] A. Kolchinsky and B. D. Tracey, "Estimating mixture entropy with pairwise distances," *Entropy*, vol. 19, no. 7, p. 361, 2017.

## 9 Appendix

### 9.1 Information flow in DNNs: $I(X; T)$

Theoretically, Shannon mutual information can measure the amount of information about a sample  $X$  that can be discovered from the intermediate representations  $T$ . Hence, we can define the privacy risk of each layer  $l$  as

$$\hat{\mathcal{L}}_{(T_l, X)} := \frac{I(X; T_l)}{H(X)}, \quad (11)$$

where  $I(X; T_l)$  is the MI between  $X$  and  $T_l$ , and  $H(X)$  is the entropy of  $X$ . Note that as  $T_l$  is a function of  $X$ , then  $H(T_l) \leq H(X)$ , thus the range of  $\hat{\mathcal{L}}_{(T_l, X)}$  is between 0 to 1.

To estimate  $I(X; T_l)$  and  $H(X)$ , several approaches, including binning method [31], k-nearest neighbor algorithm (kNN) [32, 62], kernel density estimation (KDE) [32, 63], and neural network estimator [64, 65], have been proposed. We utilize KDE similar to [32] in our setting because it is fast and accurate. Following

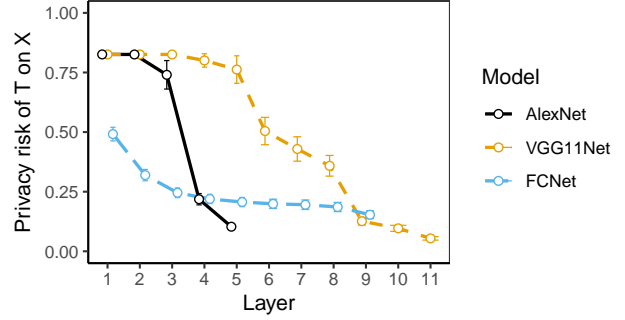


Fig. 9. Privacy risk of  $T$  on  $X$  for each layer of AlexNet, VGG11Net, and FCNet trained on LFW dataset.

KDE, the upper bound of the MI is [32, 63, 66]:

$$I(X; T_l) \leq -\frac{1}{N_{\mathcal{X}}} \sum_i \log_2 \frac{1}{N_{\mathcal{X}}} \sum_j \left( \frac{\|t_{l,i} - t_{l,j}\|_2^2}{2\alpha\sigma^2} \right), \quad (12)$$

where  $N_{\mathcal{X}}$  is the size of dataset,  $t_{l,i}$  and  $t_{l,j}$  are the intermediate representation of the layer  $l$  corresponding to the  $i^{\text{th}}$  and  $j^{\text{th}}$  samples in the dataset, and  $\alpha$  is 1 to satisfy the upper bound condition. KDE method uses this bound to estimate the MI [32]<sup>1</sup>.

As calculating of the true entropy for real-world datasets is not straightforward, we consider the maximum entropy that is  $H(X) = \log_2(N_{\mathcal{X}})$  for calculating the  $\hat{\mathcal{L}}_{(T_l, X)}$ .

Figure 9 shows the value of  $\hat{\mathcal{L}}_{(T_l, X)}$  for three state-of-the-art neural networks (AlexNet, VGG11Net, and FCNet) that are trained on LFW dataset, where  $N_{\mathcal{X}} = 9315$ . The results show that the privacy risk of  $T$  on  $X$  decreases along as we move to the latter layers. That is,  $T$  of a former layer contains more (private) information about the original input, which can be discovered by attacks for data reconstruction, etc. However, here we only evaluate on  $T$  rather than  $G$ . According to the backward Markov chain in Figure 1, only when  $W$  and  $B$  do not contain information about  $X$  (e.g., just after the initialization of model parameters in the first training step), we may be able to use the privacy risk of  $T$  on  $X$  to estimate that of  $G$  on  $X$ .

### 9.2 Attack results on $X$

We show data reconstruction attack [9, 18] results when only several layers are accessible. More specifically, Deep leakage from gradients (DLG) is a method proposed to

1 If we set  $\alpha = 4$  then we achieve the lower bound on MI



**Fig. 10.** Data reconstruction attack on different sets of layers' gradients (e.g., 1, 2, 3, 4 refer to using gradients of layer 1<sup>st</sup>, 2<sup>nd</sup>, 3<sup>rd</sup>, 4<sup>th</sup> to conduct the attack).

recover an image or tests in pixel-level or token-level [9] when observing only its gradient descents during backward propagation. Using a differentiable model, an attacker updates its dummy inputs and labels to minimize the gradients distance. When the optimization finishes, the attacker can obtain the training set from dummy inputs and labels. [18] improved DLG (iDLG) by extracting ground-truth labels firstly, and in this way, their algorithm converges quicker. To understand how gradients of different layers leak private information on  $X$ , we conduct iDLG on (1) each layer's gradients separately and (2) different sets of layers' gradients. Here we follow their paper, using CIFAR100 dataset and a different DNN model with seven Conv layers (the number of filters is 12 with the size of 5) and one FC layer (768 neurons) in the end. The results are in Figure 10). The results show that gradients of the first layer tend to be the most important one for a successful reconstruction; that is, the privacy risk of the first layer's G on original data  $X$  is the highest among the model.

### 9.3 Theoretical basis of $\mathcal{V}$ -information

The  $\mathcal{V}$ -information is introduced [38] as a new notion of information theory for a practical situation that is under computational constraints. Without putting a constraint on the type of the functions that can be used (the

*predictive family*), the  $\mathcal{V}$ -information is equivalent to the Shannon mutual information. Assuming some computational constraints for the attacker is a realistic assumption, which is the core of the many practical cryptographic systems. As a consequence, the Data Processing Inequality does not hold anymore in  $\mathcal{V}$ -information, which means processing data  $X$  can create some *usable* information. In our setting, we use  $\mathcal{V}$ -information to quantify the usable information that is contained in layers of the neural network. Here we briefly summarize the definitions and assumptions underlying the  $\mathcal{V}$ -information. For a full review, we refer to [38].

The setting is as follows: a computationally bounded agent (in our applications the adversary), is trying to predict the outcome of a real-valued random variable  $Y$  (the true value of the private feature) using another real-valued random variable  $X$  as side information (the gradient of the DNN layer). Let  $\mathcal{X}$  and  $\mathcal{Y}$  denote the sample spaces of  $X$  and  $Y$ , respectively and let  $\mathcal{P}(\mathcal{X})$  and  $\mathcal{P}(\mathcal{Y})$  denote the probability measures on  $\mathcal{X}$  and  $\mathcal{Y}$ , respectively. Furthermore, let  $f : \mathcal{X} \times \{\emptyset\} \rightarrow (\mathcal{Y})$ . In other words,  $f[x]$  ( $f[\emptyset]$ ) is a probability measure on  $\mathcal{Y}$  chosen based on the received side information  $x$  (or no side information  $\emptyset$ ). Then,  $f[x](y) \in \mathbb{R}$  is the value of the density evaluated at  $y \in \mathcal{Y}$ .

The first definition we need is that of a predictive family. Specifically, we assume that the set of models that the agent is able to use due to computational constraints,  $\mathcal{V}$ , is a predictive family defined as follows:

**Definition 1.**  $\mathcal{V}$  is a predictive family if for any  $f \in \mathcal{V}$  and  $P \in \text{range}(f)$  there exists an  $f' \in \mathcal{V}$  such that for any  $x \in \mathcal{X}$ ,  $f'[x] = P$  and  $f'[\emptyset] = P$ .

The assumption that  $\mathcal{V}$  is a predictive family is referred to as optional ignorance and guarantees non-negativity of the  $\mathcal{V}$ -information.

The  $\mathcal{V}$ -information is then defined as follows:

**Definition 2.** Let  $X$  and  $Y$  be two random variables taking values in  $\mathcal{X} \times \mathcal{Y}$ , and  $\mathcal{V}$  is a predictive family. The predictive  $\mathcal{V}$ -information from  $X$  to  $Y$  is defined as,

$$I_{\mathcal{V}}(X \rightarrow Y) = \inf_{f \in \mathcal{V}} \mathbb{E}_{y \sim Y} [-\log f[\emptyset](y)] \\ - \inf_{f \in \mathcal{V}} \mathbb{E}_{x, y \sim X, Y} [-\log f[x](y)].$$

Intuitively, it is the difference between the expected value of the predictive distribution based on side information and the expected value of the predictive distribution based on no additional information. It thus quantifies the value of adding side-information  $x$  into

the model. To estimate it numerically we can use,

$$\begin{aligned} \hat{I}_{\mathcal{V}}(X \rightarrow Y; \mathcal{D}) &= \inf_{f \in \mathcal{V}} \frac{1}{|\mathcal{D}|} \sum_{y_i \in \mathcal{D}} -\log f[\emptyset](y_i) \\ &\quad - \inf_{f \in \mathcal{V}} \frac{1}{|\mathcal{D}|} \sum_{x_i, y_i \in \mathcal{D}} -\log f[x_i](y_i), \end{aligned} \quad (13)$$

where  $f$  is one function in  $\mathcal{V}$ . A neural network can satisfy the definition of a predictive family, done by setting obtain inf, we can use gradient descent approaches such as SGD or Adam to adjust parameters in  $f$  (i.e., weights of the DNN model) similar to [38].

## 9.4 Relationship between sensitivity and $\mathcal{V}$ -information

Here we give a brief sketch of a relationship between sensitivity and  $\mathcal{V}$ -information. By a first-order Taylor approximation, viewing  $f$  as a function of a variable  $g$  which could also be  $\emptyset$ ,

$$f[g](p) = f[\emptyset](p) + \left. \frac{\partial f[g]}{g} \right|_{\emptyset} (g - \emptyset), \quad (14)$$

so that the  $\hat{I}_{\mathcal{V}}(G_l \rightarrow P; D)$  can be rewritten as,

$$\inf_{f_{\mathcal{A}} \in \mathcal{V}_{\mathcal{A}}} \frac{1}{|\mathcal{D}|} \sum_{g_{l,i}, p_i \in \mathcal{D}} -\log \left( \left. \frac{\partial f_{\mathcal{A}}[g_{l,i}]}{g_{l,i}} \right|_{\emptyset} (g_{l,i} - \emptyset) \right). \quad (15)$$

Combining this with Equation (8) we obtain that the  $\mathcal{V}$ -information is high if  $\frac{\partial z(g_{l,i})}{\partial g_{l,i}}$  is high, or in other words, if the model of the adversary is very sensitive to changes in the gradients. We assumed the adversary had access to the gradients of the DNN used for the FL model. The adversary trained its (binary classification) model on a dataset  $(g_{l,i}, p_i)$  where the  $g_{l,i}$  were obtained by passing certain data with the presence of the property being  $p_i$  through a model which had gradients  $g_{l,i}$ . Remember that the sensitivity of gradients w.r.t. the FL model output  $\mathbf{y}$  is similar to that w.r.t. the presence of the property  $\mathbf{p}$  since both are high-level information. By this construction we can only expect  $\frac{\partial z(g_{l,i})}{\partial g_{l,i}}$  to be high if  $\frac{\partial \mathbf{g}_l(\mathbf{y})}{\partial \mathbf{p}}$  is high, which in turn is high if  $\frac{\partial \mathbf{g}_l(\mathbf{y})}{\partial \mathbf{y}}$  i.e. if the sensitivity of the dataset consisting of  $\mathbf{g}_l(\mathbf{y})$  on which the adversary trained its model was sensitive to the the FL model output  $\mathbf{y}$ .